Original Research

STAT3 contributes to cisplatin resistance, modulating EMT markers, and the mTOR signaling in lung adenocarcinoma☆,☆☆ CrossMark

Ana Paula Morelli[a]; Tharcísio Citrângulo Tortelli Jr[b]; Mariana Camargo Silva Mancini[a]; Isadora Carolina Betim Pavan[a,c]; Luiz Guilherme Salvino Silva[a]; Matheus Brandemarte Severino[a]; Daniela Campos Granato[d]; Nathalie Fortes Pestana[a]; Luis Gustavo Saboia Ponte[a]; Guilherme Francisco Peruca[e]; Bianca Alves Pauletti[d]; Daniel Francisco Guimarães dos Santos Jr[a]; Leandro Pereira de Moura[e]; Rosângela Maria Neves Bezerra[a]; Adriana Franco Paes Leme[d]; Roger Chammas[b]; Fernando Moreira Simabuco[a,*]

[a] Multidisciplinary Laboratory of Food and Health, School of Applied Sciences, State University of Campinas, Limeira, SP, Brazil
[b] Centro de Investigação Translacional em Oncologia, Departamento de Radiologia e Oncologia, Faculdade de Medicina da Universidade de São Paulo and Instituto do Câncer do Estado de São Paulo, São Paulo, SP, Brazil
[c] Laboratory of Signaling Mechanisms, School of Pharmaceutical Sciences, State University of Campinas, Campinas, SP, Brazil
[d] Laboratório Nacional de Biociências (LNBio), Centro Nacional de Pesquisa em Energia e Materiais (CNPEM), Campinas, Brazil
[e] Exercise Cell Biology Laboratory, School of Applied Sciences, State University of Campinas, Limeira, SP, Brazil

Abstract

Lung cancer is the second leading cause of cancer death worldwide and is strongly associated with cisplatin resistance. The transcription factor signal transducer and activator of transcription 3 (STAT3) is constitutively activated in cancer cells and coordinates critical cellular processes as survival, self-renewal, and inflammation. In several types of cancer, STAT3 controls the development, immunogenicity, and malignant behavior of tumor cells while it dictates the responsiveness to radio- and chemotherapy. It is known that STAT3 phosphorylation at Ser727 by mechanistic target of rapamycin (mTOR) is necessary for its maximal activation, but the crosstalk between STAT3 and mTOR signaling in cisplatin resistance remains elusive. In this study, using a proteomic approach, we revealed important targets and signaling pathways altered in cisplatin-resistant A549 lung adenocarcinoma cells. STAT3 had increased expression in a resistance context, which can be associated with a poor prognosis. STAT3 knockout (SKO) resulted in a decreased mesenchymal phenotype in A549 cells, observed by clonogenic potential and by the expression of epithelial-mesenchymal transition markers. Importantly, SKO cells did not acquire the mTOR pathway overactivation induced by cisplatin resistance. Consistently, SKO cells were more responsive to mTOR inhibition by rapamycin and presented impairment of the feedback activation loop in Akt. Therefore, rapamycin was even more potent in inhibiting the clonogenic potential in SKO cells and sensitized to cisplatin treatment. Mechanistically, STAT3 partially coordinated the cisplatin resistance phenotype via the mTOR pathway in non-small cell lung cancer. Thus, our findings reveal important targets and highlight the significance of the crosstalk between STAT3 and mTOR signaling in cisplatin resistance. The synergic inhibition of STAT3 and mTOR potentially unveil a potential mechanism of synthetic lethality to be explored for human lung cancer treatment.

Introduction

Lung cancer is the leading cause of cancer death worldwide, with an estimated 1.8 million deaths in 2020 and a 5-y survival rate ranging between 10% and 20% in most countries [1]. Non-small cell lung cancer (NSCLC) is the most common type of lung cancer and lung adenocarcinoma (LUAD) is the most frequent histological subtype of the disease [2]. It is known that intrinsic molecular features in NSCLC can lead these tumors to a poor outcome [3], especially by intrinsic, adaptive, and acquired resistance to treatment [4]. While some tumors fail to respond initially, the acquired resistance is a combination of previous genetic alterations with selective alterations imposed by the treatment of choice [3]. The acquired resistance to cisplatin is mainly characterized by genetic and epigenetic alterations in the machinery of cell death and signal transduction pathways that normally lead to apoptosis in response to DNA damage [5].

Signal transducer and activator of transcription 3 (STAT3) is a transcription factor that coordinates several biological functions, including tumor cell proliferation, survival, self-renewal, tumor invasion, angiogenesis, and immunogenicity [6]. STAT3 is phosphorylated at tyrosine 705 and serine 727 in response to several growth factors, hormones, cytokines, and protein kinases [7] and remains constitutively activated in several types of cancer to sustain a malignant tumor behavior [8]. It is well documented that STAT3 is involved in radioresistance and chemoresistance [9,10], as long as the mechanistic target of rapamycin (mTOR) signaling. Liang et al reported that the hyperactivated mTORC1 signaling pathway drives chemotherapy resistance in KRAS-mutant lung cancer cells [11]. The mTOR inhibition restores chemotherapy sensitivity to cisplatin and pemetrexed in 2D and 3D cell culture, and xenograft mice models, defining mTOR inhibition as a rational therapy approach in combination with cisplatin [11]. Furthermore, a study reported that STAT3 is efficiently phosphorylated on serine 727 by the mTOR to ensures its maximal activation [12].

To assess whether mTOR is involved in STAT3 effects during cisplatin resistance, we used a CRISPR approach to abrogate STAT3 expression in A549 NSCLC cells. With a combination of quantitative proteomics, CRISPR-mediated knockout, and functional assays, we characterized that the lack of STAT3 confers an epithelial phenotype, less clonogenic survival, and sensitizes to cisplatin while reducing the mTOR pathway activation. STAT3 knockout (SKO) sensitizes to mTOR inhibition, showing that the synergistic inhibition of STAT3 and mTOR could be a potential strategy against lung cancer.

Materials and methods

Cell culture

A549 cells were maintained in HAM-F12 containing 10% fetal bovine serum (Gibco; Thermo Fisher Scientific, Inc.), penicillin (100 U/mL), and streptomycin (100 μg/mL). Cells were incubated at 37 °C with 10 μM of cisplatin (Sigma-Aldrich; Merck) for 72 h to generate the resistant condition (CisR).

Stable isotope labeling by amino acids in cell culture (SILAC) and LC-MS/MS data processing

For heavy (H)- or light (L)-lysine labeling experiments, A549 cells were maintained in a T25 flask with SILAC HAM-F12 medium (Thermo Fisher Scientific, Inc.) supplemented with 10% dialyzed FBS without lysine and arginine. The isotopic label incorporation, trypsin digestion, mass spectrometry analysis, and LC-MS/MS data processing were performed as previously described [13]. Three replicates of the experiment were performed. For statistical analysis of SILAC proteomic data, the normalized ratios H/L were converted into log2 and Student's unpaired t test was applied in the control (CTL) and cisplatin-treated (CisR) data to determine significant differentially expressed proteins ($P < 0.05$).

Bioinformatics analysis

Volcano plots were illustrated to each replicate separately using the GraphPad Prism 8.01 software (https://www.graphpad.com/) considering $P < 0.05$ [$\log_{10}(0.05) = 1.3010$] and log2 ratio $> \pm 0.25$ (fold change of CTLxCisR ratio H/L normalized). Venn diagrams were generated using InteractiVenn (http://www.interactivenn.net/) [14]. The proteins that passed the P value and FC cutoffs ($P < 0.05$ and $> \pm 0.25$, respectively) were submitted to analysis in gene ontology (GO) annotation of biological processes and proteome networks construction. Proteome networks were generated using the GENEMANIA [15] considering as valid: physical, predicted, and genetic interactions (https://genemania.org). GO classification was yielded using DAVID for biological processes [16]. The top 18 biological processes were chosen and grouped according to P value and Fold Enrichment. The raw data and parameters of DAVID analysis are available in supplementary Table S2.

Association of STAT3 gene expression with clinical outcome using database repositories

Overall survival and disease-free survival rates of patients with LUAD and lung squamous cell carcinoma were assessed using GEPIA software considering the first and third quartiles of *STAT3*, *LMNA*, *FAS*, *FDXR*, *TP53I3*, and *PCNA* expression. Hazards ratio calculation was based on Cox PH Model and considering 95% confidence interval as dotted line [17].

STAT3 knockout establishment using CRISPR/Cas9 system

To generate the SKO cells, a sgRNA sequence was designed using CRISPOR [18]. The chosen sequence used in this study was 5′-AGATTGCCCGGATTGTGGCC-3′. Oligos containing the sequence were cloned into the PX459 vector (SpCas9(BB)-2A-Puro V2.0, Addgene #62988), transfected in A549 cells using 1000 ng DNA and lipofectamine + Plus reagent (Thermo Scientific), and cultured with 1 μg/mL puromycin for 72 h for transfected cells selection. To analyze the plasmid efficiency, we performed the T7 endonuclease assay as previously described [19]. Individual transfected cells were then isolated into 96-well plates by seeding cells at low density using serial dilutions. The resulting monoclonal cultures were screened by western blot for the loss of STAT3 expression using a STAT3 antibody (Cell Signaling Technology #9139). For verification of positive monoclonal cell lines, the targeted genomic region for STAT3 was amplified by PCR from genomic DNA and sequenced. To assess the sequence of alleles, the PCR-amplified target genomic region was cloned into pGEM-T (Promega, #A3600) and clones were sequenced for SKO. Monoclonal

transfected cells with empty PX459 were used as control. The primers used for genomic screening and identification of STAT3 alleles were:

```
STAT3_genomic_F: 5'-GTTACAGAAATAGTAACGACCTCCCCTTC-3';
STAT3_genomic_R: 5'-ACTTTTAAACCATTGGGTCTGTTGGATTC-3'.
```

MTT viability assay

A549 WT and SKO cells were seeded in 96-well plates at a density of 6×10^3 cells/well for the CTL group (sensitive cells) and 1.2×10^4 cells/well for the CisR (resistant cells). To analyze IC50 and cisplatin sensitivity, cells were treated with subsequent concentrations of cisplatin (range between 5 and 50 μM). To analyze the cisplatin sensitivity induced by rapamycin (Sigma-Aldrich; Merck), we performed a previous treatment with 100 nM rapamycin in both CTL and CisR groups. After treatment, 12 mM MTT solution was added to each well for 2 h. The culture medium was aspirated and the formazan crystals were solubilized with a solution of 1 M HCl: isopropanol (1:25) for 15 min at room temperature (RT), and the absorbance was measured at 570 nm.

Clonogenic assay

A549 WT and SKO cells were seeded at low density in 6-well plates (2×10^2 cells/well) and incubated for 9 d. To analyze rapamycin effects, after seeding, the cells were treated with 100 nM rapamycin for 24 and 72 h and cultured in HAM-F12 for more than 6 to 8 d until staining. After incubation, cells were washed with PBS and stained with 1 mL of violet crystal solution (0.05% violet crystal, 1% formaldehyde, 1% methanol in PBS 1×) for 30 min in agitation at RT. The plates were washed with deionized water and colonies were counted using ImageJ software v1.53 (National Institutes of Health), converting photos into 8-bit binary pictures and considering colonies with the following size ranges: lower than 1 pixel², between 1 and 25 pixel² and greater than 25 pixel².

Western blot

Protein extracts were obtained using a lysis buffer (50 mM Tris-Cl pH 7.5, 150 mM NaCl, 1 mM EDTA, 1% Triton X-100, protease inhibitor cocktail, and phosphatase inhibitor cocktail) and samples containing 20 to 40 μg of total protein were separated by SDS-PAGE (8 and 10% acrylamide gels). The gels were electrotransferred to 0.45-μm nitrocellulose membranes (Bio-Rad Laboratories, Inc.) and incubated for 1 h at RT with 5% nonfat powdered milk dissolved in TBS-Tween-20 (TBST; 50 mM Tris-HCl, pH 7.5; 150 mM NaCl; 0.1% Tween-20). Primary antibodies were incubated overnight at 4 °C and secondary antibodies for 1 h at room temperature. Protein bands were visualized using Pierce ECL Western Blotting Substrate (Thermo Fisher Scientific, Inc.) or Clarity Max Western ECL substrate (1705063, Bio-Rad) in ChemiDoc Imaging System (Bio-Rad Laboratories, Inc.) and densitometry was performed using ImageJ software v1.53. Primary antibodies mTOR (#2972), phospho-mTOR (#2971), p70-S6K1 (#2708), phospho-p70-S6K1 (Thr389; #9234), S6 (#2317), phospho-S6 (Ser240/244; #2215), GAPDH (#2118), E-cadherin (#3195), N-Cadherin (#13116), Akt (#4685), phospho-Akt (Ser473; #4060), p53 (#2524), STAT3 (#9139), phospho-STAT3 (Tyr705; #9145), PCNA (#2586), BRCA1 (#14823), phospho-CHK1 (Ser345; #2348), phospho-CHK2 (Thr68; #2197), and Ku70 (#4588) were purchased from Cell Signaling Technology. α-Tubulin was purchased from Calbiochem (CP06), Lamin A/C from Bethyl (A303-430A), and STAT1 and Vimentin (SC-5565) from Santa Cruz Biotechnology. All antibodies were used 1:2000. Secondary antibodies: HRP-conjugated goat antimouse IgG (Sigma-Aldrich; AP308P; 1:2000) and goat antirabbit IgG (Sigma-Aldrich; AP307P; 1:5000).

Immunofluorescence

A549 WT cells were seeded on coverslips previously immersed in 6 M chloride acid solution (overnight at RT) in 24-well plates and, after 24 h, were treated with 10 μM cisplatin for 72 h. Briefly, cells were incubated with paraformaldehyde (3.7% in PBS 1 ×) for 15 min at RT, washed with PBS 1×, permeabilized with 0.5% Triton X-100 at RT for 10 min, and incubated with a blocking solution for 30 min (0.2% Triton X-100; 3% bovine serum albumin (BSA) in PBS 1×). The cells were incubated with primary antibodies mouse anti-STAT3 (1:1000; Cell Signaling #9139) and rabbit antiphospho STAT3 (Tyr705) (1:100; Cell Signaling #9145) overnight at 4°C. The cells were washed 3 times with PBS and incubated with the secondary antibodies donkey antirabbit Alexa Fluor 488 (#A21206) and donkey antimouse Alexa Fluor 568 (#A10037) (Thermo Scientific) 1:1000 for 1 h. For nuclei staining, the cells were incubated with Hoechst (10 μg/mL in PBS 1×) for 10 min. Coverslips were maintained in slides using glycerol.

Reverse transcription real-time PCR (RT-qPCR)

Total RNA was extracted from A549 WT and SKO cells using TRIzol (Invitrogen; Thermo Fisher Scientific, Inc.). The cDNA was synthesized using the High Capacity cDNA Reverse Transcription kit (Thermo Fisher Scientific, Inc.) with 2000 ng of total RNA. The qPCR reaction was performed with SYBR Green PCR Master Mix (Applied Biosystems; Thermo Fisher Scientific, Inc.) and the quantitative differences in mRNA expression were calculated according to the comparative threshold (Ct) cycle method using β-actin as the housekeeping gene. Samples were run in the Step One Plus Real-Time PCR System (Applied Biosystems; Thermo Fisher Scientific, Inc.) and Primer-BLAST was used for primers design [20] (National Institutes of Health). The sequences of primers used were:

```
STAT3_fwd: 5'-GAAACAGTTGGGACCCCTGAT-3';
STAT3_rev:5'-AGCTGTCACTGTAGAGCTGATG-3';
FDXR_fwd: 5'-TTTCTCCACACAGGAGAAGACC-3';
FDXR_rev: 5'-ACAAGGCTTCCACCCTCTTTAG-3';
PCNA_fwd: 5'-TCTTCCCTTACGCAAGTCTCAG-3';
PCNA_rev: 5'-AGGAAAGTCTAGCTGGTTTCGG-3';
FAS_fwd: 5'-CAGATCTAACTTGGGGTGGCTT-3';
FAS_rev: 5'-TGTACTTCCTTTCTCTTCACCCA-3';
TP53I3_fwd: 5'-TATCCCAGAGGGATTGACCCTG-3';
TP53I3_rev: 5'-CAGCCTGAACATTTCCCACAAG-3';
CDH1_fwd: 5'-CTTCAATCCCACCACGTACAAG-3'
CDH1_rev: 5'-TATGGTGTATACAGCCTCCCAC-3'
CDH2_fwd: 5'-GCCAAGTTCCTGATATATGCCC-3'
CDH2_rev: 5'-CAACTTCTGCTGACTCCTTCAC-3'
VIM_fwd: 5'-CCCTGAACCTGAGGGAAACTA-3'
VIM_rev: 5'-GGTCATCGTGATGCTGAGAAG-3'
β-actin_fwd: 5'-GCCGCCAGCTCACCAT-3'
β-actin_rev: 5'-CCACGATGGAGGGGAAGAC-3'.
```

Statistical analysis

All data are presented as mean ± S.D. Statistical analyses were assessed using GraphPad Prism 8.0.1 software (https://www.graphpad.com/) applying Student's unpaired t test or 1-way or 2-way ANOVA followed by Tukey's or Bonferroni's posthoc test considering $*P < 0.05$, $**P < 0.01$, $***P < 0.001$, and $****P < 0.0001$ as statistically significant.
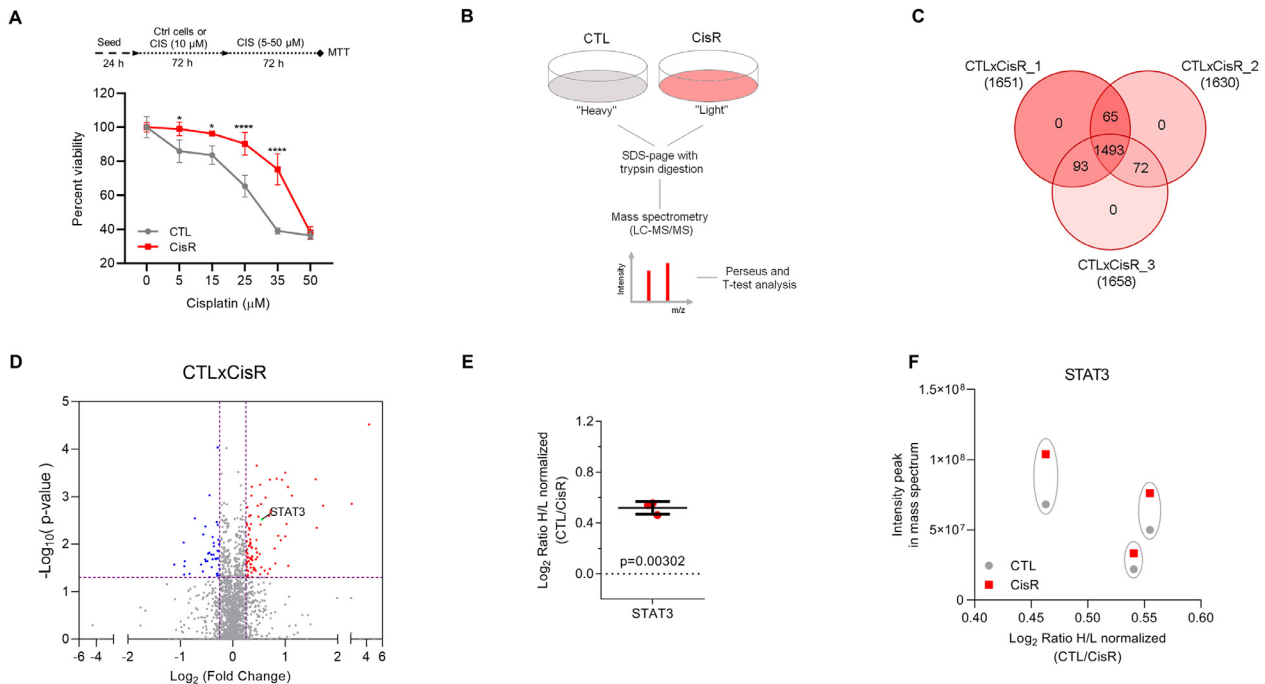
Fig. 1. SILAC proteomic analysis reveals up and downregulated targets, including STAT3, in cisplatin-resistant A549 cells. Viability assay showing that A549 cells acquired a resistant profile (CisR) after pretreatment with 10 μM cisplatin for 72 h (A). Experimental design of proteomic analysis using the stable isotope labeling by amino acids in cell culture (SILAC) approach for control (CTL) versus cisplatin-resistant cells (CisR) (B). Proteomic analysis performed in 3 replicates revealed 1651, 1630, and 1658 hits, respectively, with 1493 common altered proteins (C). A representative volcano plot displays the log2 fold change (x-axis) against the t test-derived $-\log10$ statistical P value (y-axis) (cutoffs ± 0.25 ratio H/L and $P < 0.05$, t test) for all proteins differentially expressed in CTL versus CisR A549 cells (D). Distribution of the log2 ratio H/L among the replicates of the SILAC analysis, revealing $P = 0.00302$ after t test (E). Individualized analysis of the peak intensity between the samples, comparing CTL and CisR samples of each replicate (F). Volcano plot replicates are provided in Supplementary Fig. S1.

Results

SILAC proteomic analysis reveals STAT3 as an upregulated target in cisplatin resistance A549 cells

The main objective of this study was to identify novel cisplatin resistance (CisR) biomarkers derived from diverse pathways that contribute to CisR of lung cancer. The proteomic-driven investigation started with the hypothesis that STAT3 would be involved in the CisR profile since the protein appeared with differential expression after induction of cisplatin resistance in A549 cells. The proteomic analysis comprised A549 cells pretreated with 10 μM cisplatin for 72 h for an acquired resistance profile (Fig. 1A, $n = 3$). The SILAC analysis has been previously described [21] and is summarized in Fig. 1B and the methods section. The final data set comprised 1493 quantified proteins common between 3 replicates (Fig. 1C, Supplementary Table S1). Differential expression analysis revealed 131 proteins with significantly altered levels when comparing CTL and CisR [$P < 0.05$, t test] (Fig. 1D, Supplementary Table S1 and Supplementary Fig. S1). Regarding STAT3, we can observe the distribution of the log2 ratio H/L among the replicates of the SILAC analysis, revealing $P = 0.00302$ after t test (Fig. 1E, standard deviation 0.0496, standard error mean 0.0282, coefficient of variation 9.542%). Also, the individualized analysis of the peak intensity between the samples reveals that in all samples, STAT3 is increased in CisR compared to the CTL samples (Fig. 1F).

We subsequently performed a GO classification of the 131 significantly increased or decreased proteins in the A549 CisR proteome using the DAVID software. GO analysis was expressed crossing P value [$-\log10$] and fold enrichment from DAVID analysis (Fig. 2A and B, Supplementary

Table S2) and revealed strong relationships to tumoral and resistance-related processes, such as upregulation of Wnt signaling pathway, NIK/NF-κB signaling, DNA repair, and downregulation of proteins involved in migration and splicing (Fig. 2A and B, Supplementary Table S2). Conversely, we performed a network analysis of the upregulated (Fig. 2C) and downregulated (Fig. 2D) proteins after CisR using GeneMANIA, a software that establishes interactions based on evidence of literature regarding physical, predicted, and genetic interaction between proteins. In summary, network analysis and classification of the proteome analysis yielded consistent data of lung-specific pathway alterations after CisR, including potential targets to circumvent the resistant profile: STAT3, Lamin A/C, Fas, PCNA, *FDXR* (FDXR), and *TP53I3* (PIG3). We selected STAT3 for further exploration as a critical target in cisplatin resistance.

STAT3 activation and expression are markers of poor prognosis and cisplatin resistance in lung cancer

To investigate the relationship between STAT3 and survival, we analyzed the survival rate of LUAD and lung squamous cell carcinoma patients with low or high STAT3 expression using the Gene Expression Profiling Interactive Analysis (GEPIA) database. The analysis showed that the percent of disease-free survival rates (Fig. 3A) of patients with STAT3-low expression was higher than patients with STAT3-high expression, with a hazard ratio (HR) of 1.4 ($P = 0.029$). The survival analysis of the other SILAC targets validated here is shown in Supplementary Fig. S2A. Besides, we validated potential CisR biomarkers identified in SILAC analysis using western blot and RTqPCR: STAT3, Lamin A/C, Fas, PCNA, *FDXR,* and *TP53I3*). STAT3 significantly presented increased protein content and phosphorylation at Y705 in CisR
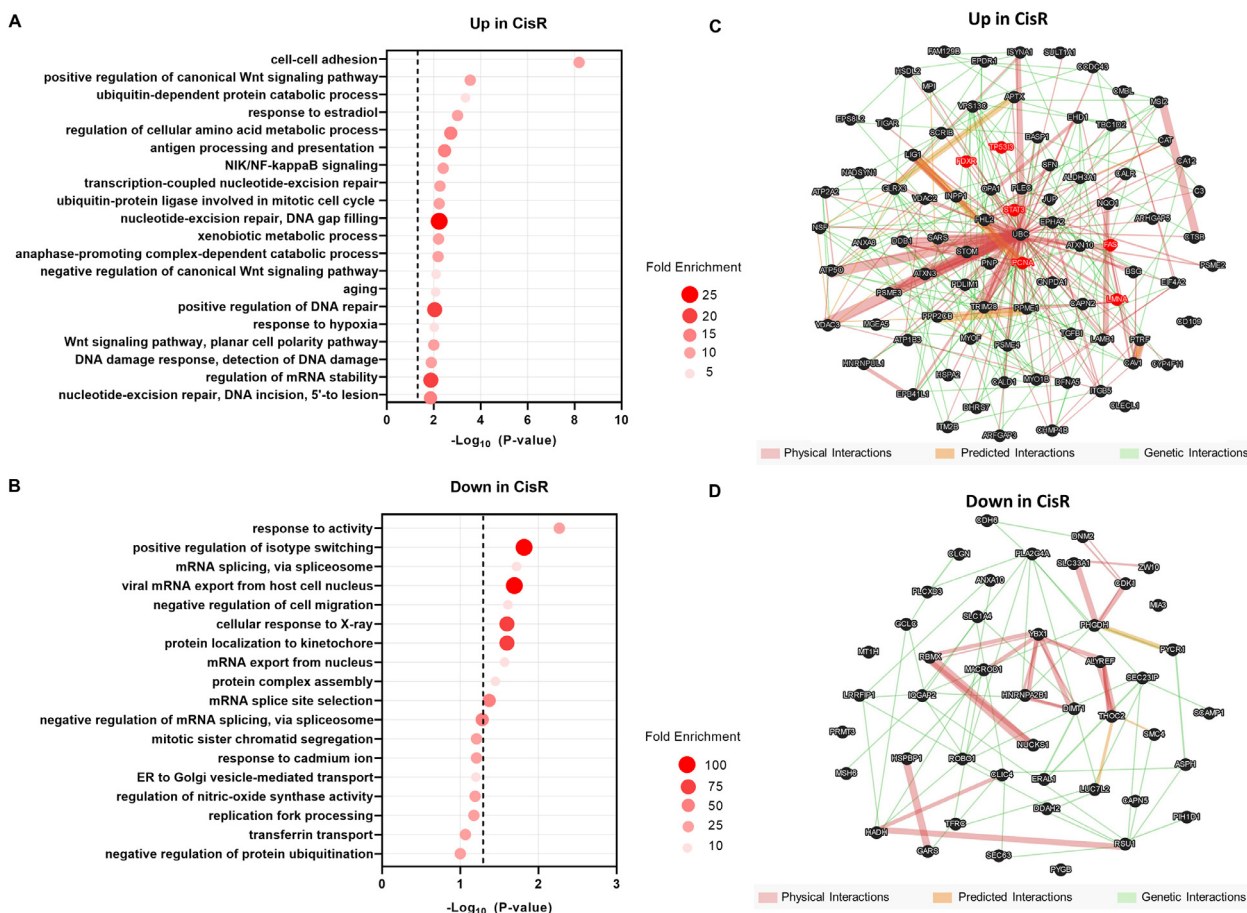
Fig. 2. Biological classification and network analysis link important targets up and downregulated in cisplatin-resistant (CisR) A549 cells. Top 18 biological processes (BP) by gene ontology (GO) classification on DAVID platform is shown for proteins with significantly increased (up in CisR) or decreased (down in CisR) levels in cisplatin-resistant cells (±0.25 ratio H/L with $P< 0.05$), both ranked according to $-\log10$ statistical P value (x-axis) and fold enrichment of each BP (size of circles) (A, B). The DAVID analysis parameters are described in Supplementary Table S2. The targets and their interactions were analyzed through GENEMANIA, showing physical interactions (pink), predicted interactions (orange), and genetic interactions (green) (C, D). Proteins validated by RTqPCR and western blot are highlighted in red. (For interpretation of the references to color in this figure legend, the reader is referred to the Web version of this article.)

cells (Fig. 3B and C). Other targets also had significantly increased protein levels after CisR, including Fas, PCNA, and Lamin A (Fig. 3B and C). Consistent with protein levels, the immunostaining reveals more p-STAT3 fluorescence intensity (Fig. 3D and E, Supplementary Fig. S2). Besides, STAT3 mRNA was increased in A549 CisR cells (CTL mean = 1.1015; CisR mean = 3.049, p=0.006, Fig. 3G) and *FDXR, FAS, PCNA*, and *TP53I3* also presented increased mRNA levels after CisR (Fig. 3G). These results confirmed the proteomic findings and suggest that STAT3 high expression is a potential marker for poor prognosis and CisR in lung cancer.

Generation of A549 STAT3 knockout cells

To analyze the role of STAT3 in CisR profile, we employed CRISPR/Cas9 gene editing to introduce genomic mutations in the STAT3 gene in A549 cells. We constructed the plasmid by cloning the synthesized sgRNA sequence for STAT3 (Supplementary Fig. S3A, primers available on methods) and validated the Indels generation efficiency through the T7 endonuclease I assay after the transfection of the construct. The efficiency obtained in polyclonal A549 cell cultures (mixed population) transfected with the construct was 31.17% (Supplementary Fig. S3B). Polyclonal cultures were initially screened for the loss of STAT3 expression by western blot using a specific antibody against total STAT3 (Supplementary Fig. S3C and S4A) and then subjected to clone isolation. Two resulting cell clones, termed SKO 22 and 28, were chosen for further validation (Supplementary Fig. S4B). SKO 22 was sequenced (Supplementary Fig. S3D), as well as 2 possible off-targets, ensuring the specific modification in STAT3 through the CRISPR/Cas9 system (Supplementary Fig. S4C). Decomposition of the genomic sequencing through TIDE software confirmed that STAT3 alleles were heterozygous, edited with an efficiency of 93.7 ($R^2 = 0.94$), and with 3 probably types of indels (+1, +3, and +10 nucleotides, $P< 0.001$, supplementary Fig. S3E). TA cloning of the PCR-amplified target region and Sanger sequencing revealed 2 types of alleles found in the TIDE analysis (+1 and +10 indels), confirming the heterozygous genotype of this SKO cell clone (Supplementary Fig. S3F and S4D). Thus SKO 22 was used for subsequent experiments.

STAT3 gene disruption impairs clonogenic survival and mesenchymal phenotype in A549 cells

As expected, the SKO A549 cell line exhibited a residual mRNA expression (mean 0.23, $P= 0.0022$, Fig. 4A), but presented loss of STAT3 expression and phosphorylation (Fig. 4B). STAT3 KO increased STAT1
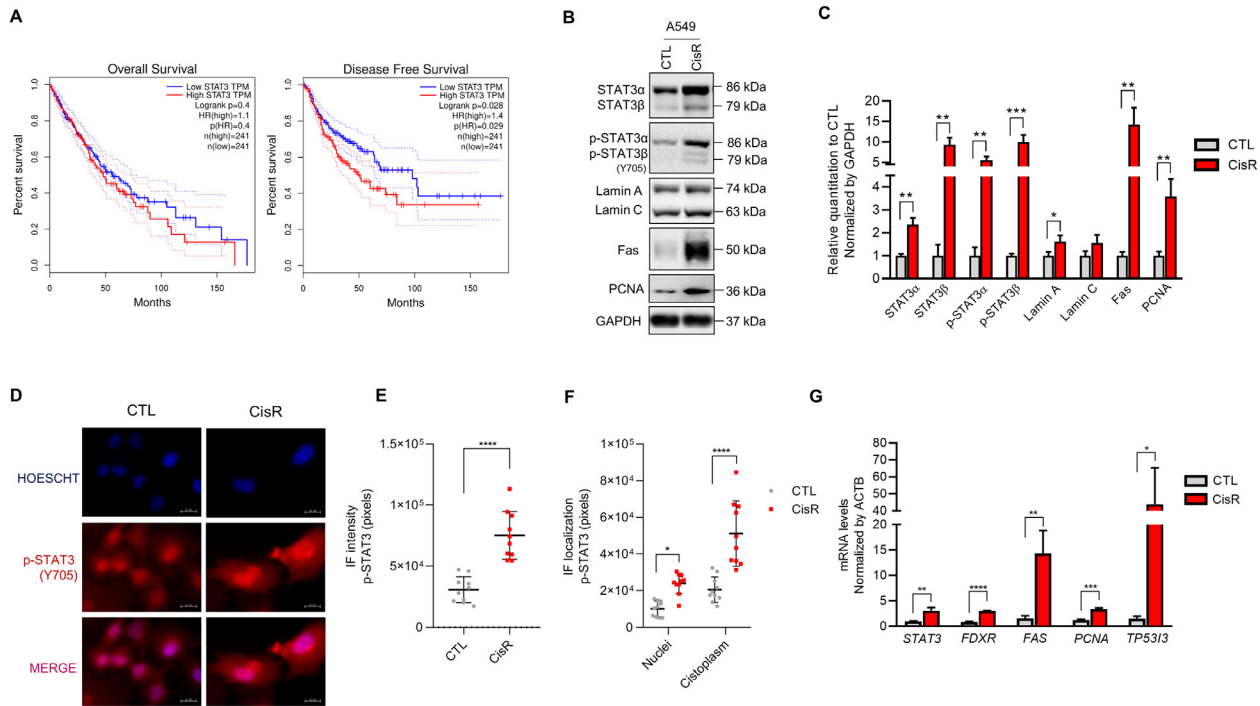
Fig. 3. Validation of targets from SILAC analysis, including STAT3, which has poor lung cancer prognosis and is predominantly nuclear in CisR A549 cells. Overall and disease-free survival analysis performed in the GEPIA platform revealed a decreased survival in lung adenocarcinoma (LUAD) and lung squamous carcinoma (LUSC) patient samples with high STAT3 expression (A). Western blotting (B, C) and RTqPCR (E) analyzes confirm the increased protein and mRNA levels of important targets reported in SILAC analysis: STAT3, lamina A/C, Fas, *FDXR*, PCNA, and *TP53I3*. Immunofluorescence analyses of p-STAT3 and STAT3 expression in A549 cells treated with 10 μM cisplatin for 72 h with n ≥ 3 for each group with 2 biological replicates (D, E). All data represent the mean ± SD. Statistical analysis of western blot was assessed after unpaired *t* test (*$P < 0.05$; **$P < 0.01$; ***$P < 0.001$; ****$P < 0001$). Source data are provided in Supplementary Fig. S2.

expression, an effect already proposed as a therapeutic approach in esophageal squamous cancer [22] (Fig. 4B, supplementary Fig. S5A). Next, we examined the functional effects of SKO on viability and clonogenic survival of A549 cells. SKO cells presented similar viability compared to WT cells over time (Fig. 4C) and responded equally to cisplatin treatment for 72 h (Fig. 4D). Despite the absence of changes in viability and the number of colonies (Fig. 4E, Supplementary Fig. S5G), SKO cells exhibited a predominant epithelial morphology when compared to WT cells (Fig. 4E, Supplementary Fig. S5D). Furthermore, the size of colonies of SKO cells was significantly reduced compared to WT cells (Fig. 4F). SKO expressed significantly more E-cadherin and less N-Cadherin, both analyzed by western blot and RTqPCR, suggesting the acquisition of a predominant epithelial phenotype (Fig. 4G, H, and I). The raw data and the validation of the results using the SKO 28 monoclonal culture are presented in the supplementary Fig. S5.

STAT3 deficient cells do not acquire cisplatin resistance nor overactivate mTOR signaling upon cis treatment

In KRAS mutant lung cancer cells, the epithelial phenotype and the mTOR pathway activation are associated with cisplatin sensitivity [[11],[23]]. SKO cells, when treated with 10 μM cisplatin for 72 h, did not acquire resistance to subsequent concentrations of cisplatin (Fig. 5A), reflecting significantly lower IC50 compared to WT cells (Fig. 5B, WT CTL mean = 19.21, SKO CTL mean = 17.49; WT CisR mean = 29.72, SKO CisR mean = 21.90; WT CisR versus SKO CisR *P*= 0.0036). We also evaluated the mTOR pathway status in both WT and SKO cells. A549 WT cells pretreated with 10 μM cisplatin showed a significant increase in mTOR

and S6 phosphorylation, which did not occur in SKO cells (Fig. 5C, D, and F). Furthermore, treatment with 30 μM cisplatin in a short time significantly increased important DNA damage markers in SKO cells, as p-CHK1 and Ku70, when compared to WT-treated cells (Fig. 5G, H, and J), suggesting an increased DNA damage response in cells with the lack of STAT3. Overall, these findings indicate that STAT3 is crucial in acquired resistance to cisplatin and is directly related to the overactivation of the mTOR signaling pathway.

SKO cells are more sensitive to mTOR inhibition by rapamycin

To evaluate the combined effects between STAT3 and mTOR inhibition, SKO cells were subjected to treatment with 100 nM rapamycin for 72 h and subsequently to different concentrations of cisplatin (5–25 μM) (Fig. 6A and B). SKO cells were sensitized at 15 and 20 μM cisplatin after mTOR inhibition compared to WT cells, showing that the lack of STAT3 potentiated the effects of rapamycin in A549 cells. Moreover, it is reported that rapamycin leads to feedback activation of Akt in serine 473 [24], failing to inhibit prosurvival pathways through mTORC2–Akt pathway [25]. The inhibition of mTOR and S6 was greater in cells lacking STAT3 when compared to WT cells (Fig. 6C, E, and G). Also, the activation feedback loop in Akt (Ser473) was significantly reduced in SKO cells (Fig. 6C and D). This sensitivity is reflected by reduced clonogenic potential, after 24 and 72 h of treatment with 100 nM rapamycin (Fig. 6H, supplementary Fig. S7A), significantly reducing the number (Fig. 6I) and size of colonies formed (Fig. 6J and K). Thus, these data suggest that the STAT3 abrogation improves the responsiveness to mTOR inhibition and decreases the activation of prosurvival pathways induced by the mTORC2-Akt axis.
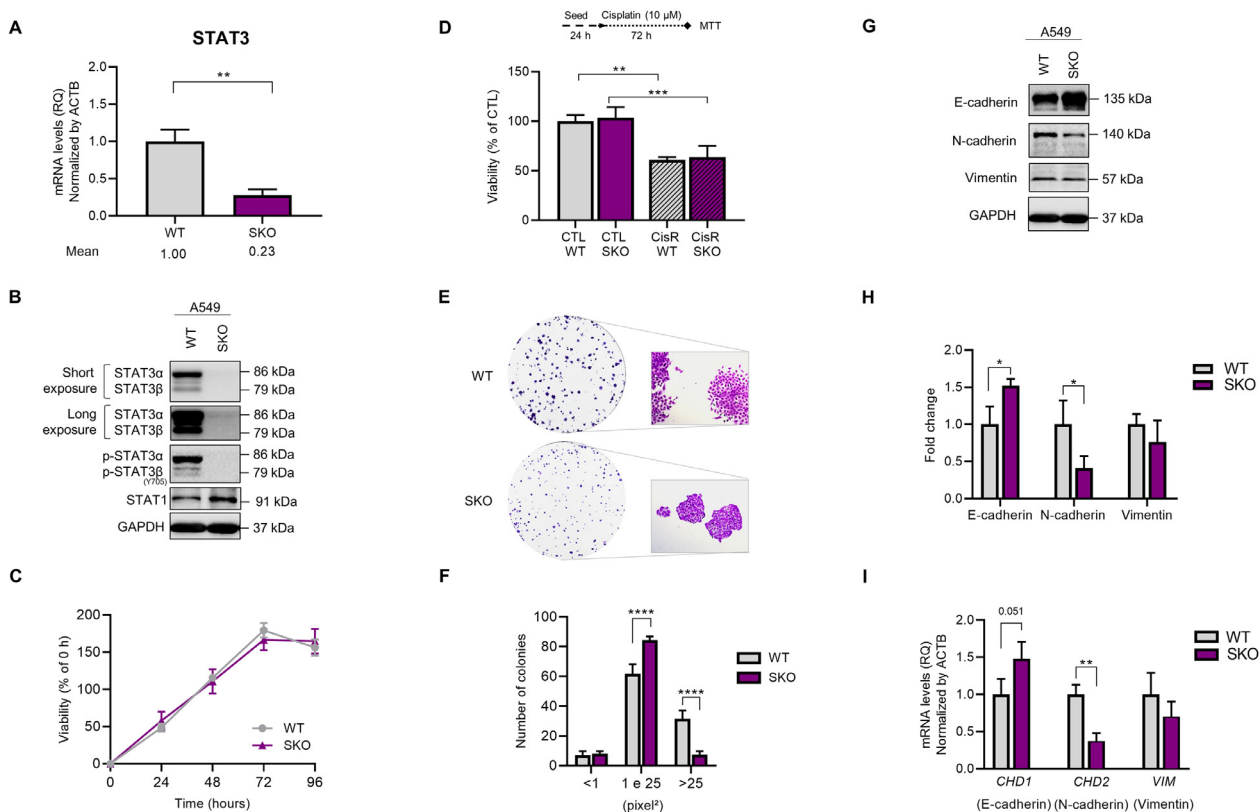
Fig. 4. STAT3 knockout decreases clonogenic potential while exhibiting an epithelial phenotype. Partial loss of STAT3 mRNA levels showed by RTqPCR (A) and western blot analysis, reporting the loss of STAT3 expression and phosphorylation (Tyr705) in A549-SKO generated through CRISPR/Cas9 gene-editing system (B). Western blot of the other obtained SKO cell clones is presented in Supplementary Fig. 4A. MTT viability assay was performed and A549 WT and KO cells showed the same viability over time (C) and after treatment with 10 μM cisplatin for 72 h (D). The clonogenic survival assay indicates an epithelial phenotype of SKO cells (E). The graph shows the size of colonies after 8 d measured using the ImageJ software (F). The mesenchymal phenotype was assessed by analyzing the EMT pathway proteins by western blotting (G, H) and RTqPCR (I). All data represent the mean ± SD. Statistical analysis of IC50 was assessed after 2-way ANOVA followed by Tukey post-test and statistical of mRNA levels and western blot was assessed after unpaired *t* test (*$P<$ 0.05; **$P<$ 0.01; ***$P<$ 0.001; ****$P<$ 0001). Raw data are provided in Supplementary Fig. S5.

Discussion

Here, we describe important targets presenting increased or decreased expression in NSCLC cisplatin resistance context. Proteomic-based approaches to identify novel targets are urgently needed to better understand and target the diverse pathways underlying chemoresistance [26]. These studies not only promise to orientate the diagnostic framework of lung cancer but also drive individualized therapeutic strategies [27,28]. As in other SILAC-based studies [[29], [30]], our analysis identified important pathways upregulated during cisplatin resistance, reflecting the control of cell-cell adhesion, antigen processing and presentation, NIK/ NF-κB signaling, Wnt signaling, DNA damage response, and activation of DNA repair pathways. The downregulated pathways especially reflected decrease of "mRNA splicing", "mRNA export from the nucleus", and "negative regulation of cell migration" (all proteins classified in each biological process are presented in the supplementary Table S2).

Galluzzi et al defined cisplatin resistance in 4 main mechanisms: (i) reduction of drug accumulation in the cytoplasm; (ii) increased interaction of cisplatin and other cytoplasmic molecules, preventing interaction with DNA; (iii) activation of repair mechanisms, as mismatch repair (MMR), nucleotide-excision repair (NER), base-excision repair (BER) and double-strand breaks repair (DSBs), and (iv) decreased apoptotic stimulus [5]. Consistent with our study, other studies reported that the bulky DNA adducts

generated by cisplatin are mainly repaired by the NER pathway [31] and the deficiency in triggering DNA repair in testis cancer cells is a determining factor for high cisplatin sensitivity [32]. Moreover, DNA repair inhibition seems to be a critical mechanism for cisplatin sensitivity in lung cancer [[33], [34]]. Here, the increased activation of Ku70 and p-CHK1 in STAT3-deficient cells (Fig. 5G) possibly indicates greater chemically-induced DSBs [35].

Our results also show the downregulation of splicing via spliceosome, an emerging biological process involved in chemoresistance [36]. We validated important MS-based targets already described as critical regulators of tumor progression and chemoresistance [37–39], including the tumor necrosis factor receptor superfamily member 6 (Fas/CD95). Fas is a surface protein that mediates the extrinsic apoptotic pathway and, in the context of cancer, CD95-mediated apoptosis has been reported [40]. Moreover, chemotherapy may maintain an antiapoptotic response by increasing the concentration of a soluble antiapoptotic isoform of Fas, generated by alternative splicing [41]. Regarding splicing, cisplatin resistance reduced the acetylation of serine-arginine protein kinase 1 (SRPK1), an upregulated kinase in NSCLC [42], favoring the splicing of some antiapoptotic variants [43]. Cisplatin also regulated the Serine/arginine-Rich Splicing Factor 2 (SRSF2) in epithelial ovarian cancer (EOC) [44]. Overall, these findings provide new possible biomarkers and targets for CisR, driving future research and clinical applications to overcome platinum resistance.
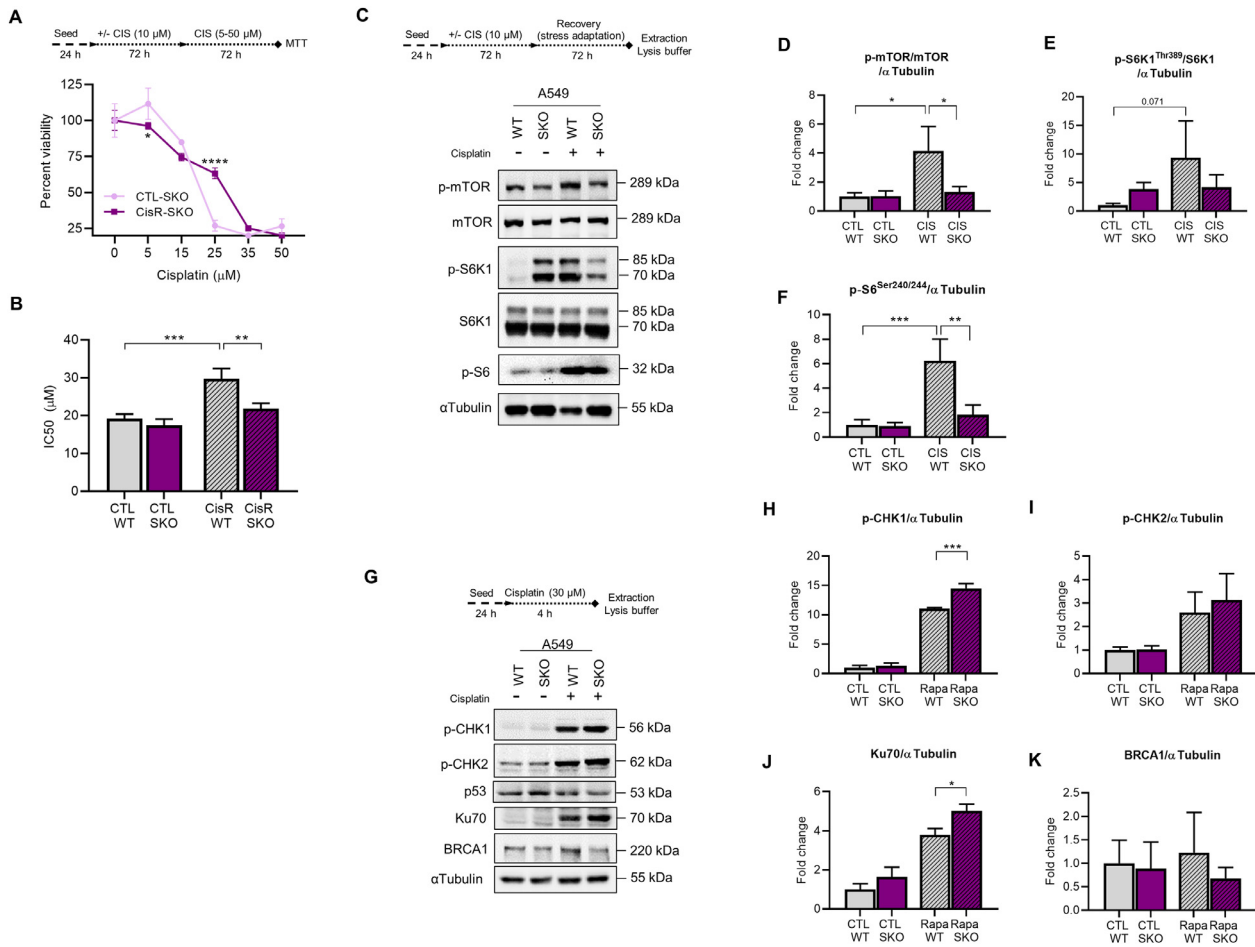
Fig. 5. SKO cells do not acquire a resistant profile while exhibiting impairment in mTOR signaling and increasing DNA-damage response. A viability assay showing that SKO cells do not acquire a resistant profile after pre-treatment with 10 μM cisplatin for 72 h, both by percent survival (A) and IC50 (B). Western blot experiment showing the increase of mTOR signaling in resistant A549 WT cells, reversed by SKO after 72 h of recovery condition (C). The graph shows bands densitometry of mTOR (D), S6K1 (E), and S6 (F). Western blot showing WT and SKO response after 30 μM cisplatin for 4 h (G). The graph shows bands densitometry of p-CHK1 (H), p-CHK2 (I), Ku70 (J), and BRCA1 (K). All data represent the mean ± SD. Statistical analysis of percent viability and clonogenic survival was accessed after 2-way ANOVA followed by Bonferroni's post-test and IC50 was assessed after 2-way ANOVA followed by Tukey's post-test. Statistical of western blot was assessed after 1-way ANOVA followed by Tukey's post-test ($*P< 0.05$; $**P< 0.01$; $***P< 0.001$; $****P< 0001$). Raw data are provided in Supplementary Fig. S6.

Importantly, literature and the MS-based proteomics analysis presented here indicate that STAT3 is a critical cisplatin resistance regulator. Persistent and aberrant STAT signaling is a recurrent feature of human cancers [45] and studies extensively reported that STAT3 signaling is involved in radiotherapeutic and chemotherapeutic sensitivity [46–48]. STAT3 is also described as an inducer of epithelial-mesenchymal transition (EMT) [49]. A recent evidence reported that phosphorylation of STAT3 at Y705 promoted cancer cell EMT and metastasis through the regulation of E-cadherin and Vimentin [50]. Accordingly, the STAT3 phosphorylation at S727 potentially resulted in cancer cell proliferation and the establishment of macroscopic colonies, while IL-6-induced phosphorylation of the STAT3 Y705 residue regulated EMT, controlling the EMT-mesenchymal-epithelial transition switch in cancer stem cells [51]. Although STAT3 is related to the EMT-mesenchymal-epithelial transition switch, this study found the predominance of an epithelial phenotype in the absence of STAT3 expression and phosphorylation in A549 cells. Collectively, these data reinforce that the phosphorylation of STAT3 at Y705 and the phosphorylation at S727 by mTOR [12] may be related to the epithelial phenotype in SKO cells.

Alternative strategies aimed at concomitantly blocking STAT3-dependent signaling with functionally related pathways have been already employed [[52],[53]]. Regarding the mTOR signaling, rapamycin potentiated cisplatin response in KRAS-mutant lung cancer, and this efficacy was correlated with mTOR activity induced by cisplatin treatment [11]. In accordance, here we propose molecular determinants that limit the efficacy of cytotoxic chemotherapy, suggesting the concomitant inhibition of STAT3 and mTOR signaling pathways as a strategy against lung cancer. Consistent with our data, the levels of STAT3 were significantly decreased when mTOR was inhibited by rapamycin [54] and STAT3 blockage enhanced apoptosis induced by PI3K and mTOR inhibition in NSCLC cells [55]. When we analyze the proteins upregulated in CisR (Fig. 2A and C), in this case considering mTOR as the input gene, we observe that STAT3 and mTOR share increased targets: BASP1, TRIM28, PSME4, and ATXN10 (data not shown). Further studies can explore this crosstalk of mTOR-STAT3 more clearly, bringing multiomic analyzes in conditions of presence and absence of STAT3 in different types of cancer. Furthermore, STAT3 knockdown sensitized to rapamycin treatment and a STAT3 inhibitor impaired mTOR activation in osteosarcoma cells [56]. The feedback activation of STAT3 also drives the
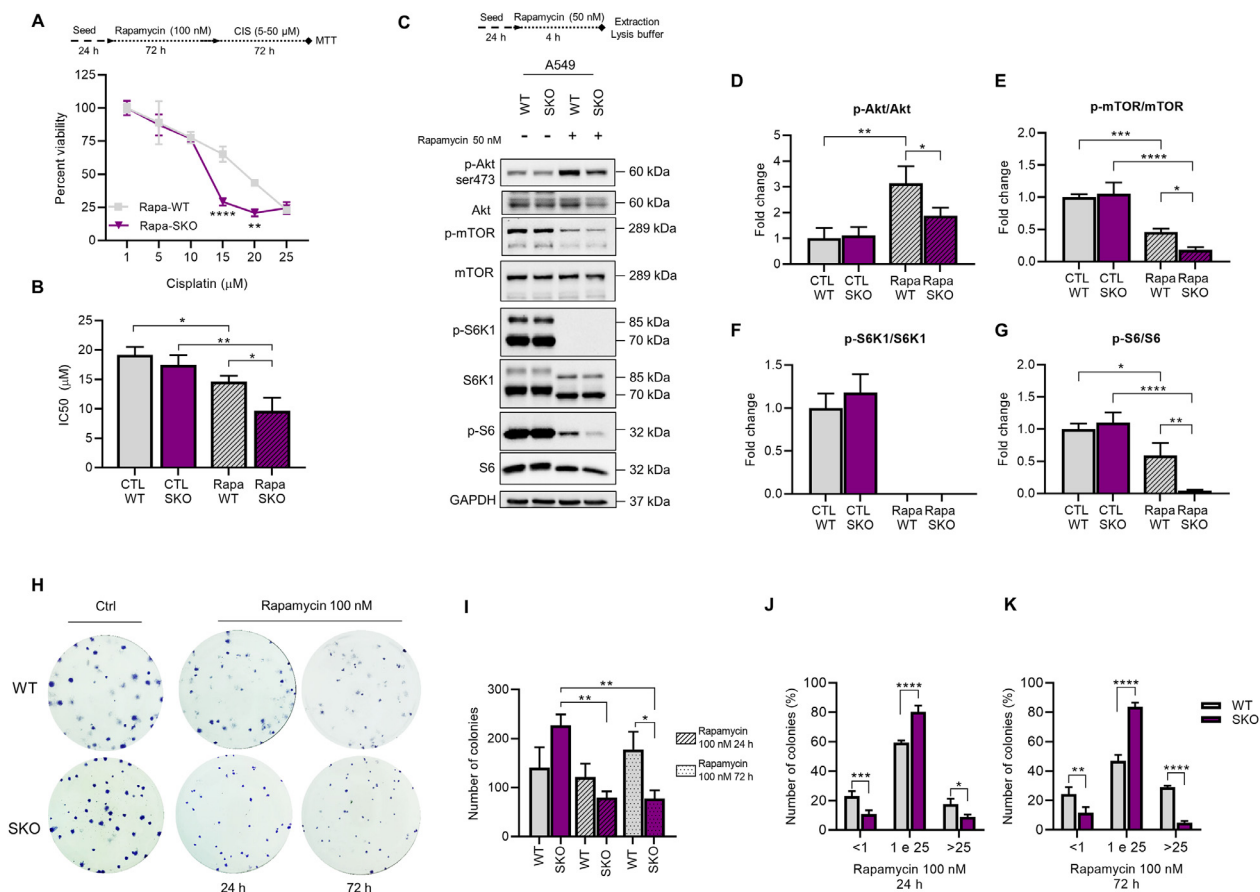
Fig. 6. SKO cells are more responsive to rapamycin and pretreatment with rapamycin sensitizes to cisplatin. A viability assay showing that pretreatment with rapamycin 100 nM for 72 h sensitize SKO cells to cisplatin, both by percent survival (A) and IC50 (B). Western blot showing the inhibition of mTOR signaling after 50 nM of rapamycin for 4 h in WT and SKO cells, with reduced Akt feedback activation loop in SKO cells (C). The graph shows bands densitometry of Akt (D), mTOR (E), S6K1 (F), and S6 (G). Treatment with 100 nM rapamycin for 24 and 72 h decreases the clonogenic survival of SKO cells (H). The graph shows the number of colonies (I) and size of colonies after 24 (J) and 72 h (K) treatment measured using the ImageJ software (F). Statistical analysis of percent viability and clonogenic survival was accessed after 2-way ANOVA followed by Bonferroni's post-test and IC50 was assessed after 2-way ANOVA followed by Tukey's post-test. Statistical of western blot was assessed after 1-way ANOVA followed by Tukey's post-test ($*P < 0.05$; $**P < 0.01$; $***P < 0.001$; $****P < 0001$). Source data are provided in Supplementary Fig. S7.

sensitivity to PI3K/AKT/mTOR inhibitors in PTEN-deficient cancer cells [57], evidencing the synergic inhibition of STAT3 and mTOR as a potential anticancer strategy. Collectively, these data suggest that mTOR and STAT3 pathways inhibition may be considered as a strategy against different types of cancer.

Conclusions

Overall, our study reports the hyperactivation of the mTOR signaling pathway as a mechanism of chemotherapy resistance in A549 lung cancer cells and identifies several other cisplatin resistance biomarkers through proteomics-based identification. Despite the use of a single cell line in this study, here we reinforce that STAT3 participates in EMT and cisplatin susceptibility, providing mechanistic support for the combination of cisplatin, rapamycin, and STAT3 abrogation as a rational therapeutic approach against lung cancer. Future studies assessing the translational effects of STAT3 and mTOR inhibition will be critical to determine the effectiveness of this potential synthetic lethality strategy for NSCLC.

Data availability

The mass spectrometry proteomics data have been deposited in the ProteomeXchange Consortium (http://proteomecentral.proteomexchange.org) via the PRIDE partner repository [58] with the data set identifier PXD025778.

Authors' contributions

Ana Paula Morelli: Conceptualization, Methodology, Validation, Formal analysis, Investigation, Writing - Original Draft, Writing - Review & Editing, Visualization. Tharcísio Citrângulo Tortelli Jr: Conceptualization, Methodology, Writing - Review & Editing. Mariana Camargo Silva Mancini: Investigation, Writing - Review & Editing. Isadora Carolina Betim Pavan: Investigation, Writing - Review & Editing. Luiz Guilherme Salvino Silva: Investigation, Writing - Review & Editing. Matheus Brandemarte Severino: Investigation, Writing - Review & Editing. Daniela Campos Granato: Validation, Formal analysis, Writing - Original Draft, Writing - Review & Editing, Visualization. Nathalie Fortes Pestana: Investigation. Luis Gustavo Saboia Ponte: Investigation, Writing - Review & Editing. Guilherme

Acknowledgments

Supplementary materials

Supplementary material associated with this article can be found, in the online version, at doi:10.1016/j.neo.2021.08.003.

References

[1] Sung H, Jacques F, Siegel RL, Laversanne M, Soerjomataram I, Jemal A, Bray F. Global cancer statistics 2020: GLOBOCAN estimates of incidence and mortality worldwide for 36 cancers in 185 countries. *CA: Cancer J Clin* 2021;**17**(2):209–49.

[2] Meza R, Meernik C, Jeon J, Cote ML. Lung cancer incidence trends by gender, race and histology in the United States, 1973-2010. *PloS One* 2015;**10**(3):e0121323.

[3] Rotow J, Bivona TG. Understanding and targeting resistance mechanisms in NSCLC. *Nat Rev Cancer* 2017;**17**(11):637–58.

[4] Bivona TG, Doebele RC. A framework for understanding and targeting residual disease in oncogene-driven solid cancers. *Nat Med* 2016;**22**(5):472–8.

[5] Galluzzi L, Senovilla L, Vitale I, Michels J, Kepp O, Castedo M, Kroemer G. Molecular mechanisms of cisplatin resistance. *Oncogene* 2012;**31**(15):1869–83.

[6] Yu H, Lee H, Herrmann A, Buettner R, Jove R. Revisiting STAT3 signalling in cancer: new and unexpected biological functions. *Nat Rev Cancer* 2014;**14**(11):736–46.

[7] Lahiri T, Brambilla L, Andrade J, Askenazi M, Ueberheide B, Levy DE. Mitochondrial STAT3 regulates antioxidant gene expression through complex I-derived NAD in triple negative breast cancer. *Mol Oncol* 2021;**15**(5):1432–49.

[8] Hu R, Han Q, Zhang J. STAT3: a key signaling molecule for converting cold to hot tumors. *Cancer Lett* 2020;**489**:29–40.

[9] Wang X, Zhang X, Qiu C, Yang N. STAT3 contributes to radioresistance in cancer. *Front Oncol* 2020;**10**:1–8.

[10] Tan FH, Putoczki TL, Stylli SS, Luwor RB. The role of STAT3 signaling in mediating tumor resistance to cancer therapy. *Curr Drug Targets* 2014;**15**(14):1341–53.

[11] Liang S-Q, Buhrer ED, Berezowska S, Marti TM, Xu D, Froment L, Yang H, Hall SRR, Vassella E, Yang Z, et al. mTOR mediates a mechanism of resistance to chemotherapy and defines a rational combination strategy to treat KRAS-mutant lung cancer. *Oncogene* 2019;**38**(5):622–36.

[12] Yokogami K, Wakisaka S, Avruch J, Reeves SA. Serine phosphorylation and maximal activation of STAT3 during CNTF signaling is mediated by the rapamycin target mTOR. *Curr Biol* 2000;**10**(1):47–50.

[13] Morelli AP, Tortelli TC Jr, Pavan ICB, Silva FR, Granato DC, Peruca GF, Pauletti BA, Domingues RR, Bezerra RMN, de Moura LP, et al. Metformin impairs cisplatin resistance effects in A549 lung cancer cells through mTOR signaling and other metabolic pathways. *Int J Oncol* 2021;**58**(6):28.

[14] Heberle H, Meirelles GV, da Silva FR, Telles GP, Minghim R. InteractiVenn: a web-based tool for the analysis of sets through Venn diagrams. *BMC Bioinform* 2015;**16**(1):169.

[15] Warde-Farley D, Donaldson SL, Comes O, Zuberi K, Bradawi R, Chao P, Franz M, Grouios C, Kazi F, Lopes CT, et al. The GeneMANIA prediction server: biological network integration for gene prioritization and predicting gene function. *Nucleic Acids Res* 2010;**38**:W214–20 Web Server issue.

[16] Huang DW, Sherman BT, Lempicki RA. Systematic and integrative analysis of large gene lists using DAVID bioinformatics resources. *Nat Protocols* 2009;**4**(1):44–57.

[17] Tang Z, Li C, Kang B, Gao G, Li C, Zhang Z. GEPIA: a web server for cancer and normal gene expression profiling and interactive analyses. *Nucleic Acids Res* 2017;**45**(W1):W98–102.

[18] Concordet J-P, Haeussler M. CRISPOR: intuitive guide selection for CRISPR/Cas9 genome editing experiments and screens. *Nucleic Acids Res* 2018;**46**(W1):W242–5.

[19] Ran FA, Hsu PD, Wright J, Agarwala V, Scott DA, Zhang F. Genome engineering using the CRISPR-Cas9 system. *Nat Protocols* 2013;**8**(11):2281–308.

[20] Ye J, Coulouris G, Zaretskaya I, Cutcutache I, Rozen S, Madden TL. Primer-BLAST: a tool to design target-specific primers for polymerase chain reaction. *BMC Bioinform* 2012;**13**:134.

[21] Mann M. Functional and quantitative proteomics using SILAC. *Nat Rev Mol Cell Biol* 2006;**7**(12):952–8.

[22] Liu Z, Zhang Y, Chen Y, Lin Y, Lin Z, Wang H. STAT1 inhibits STAT3 activation in esophageal squamous cell carcinoma. *Cancer Manage Res* 2018;**10**:6517–23.

[23] Ashrafizadeh M, Zarrabi A, Hushmandi K, Kalantari M, Mohammadinejad R, Javaheri T, Sethi G. Association of the epithelial-mesenchymal transition (EMT) with cisplatin resistance. *Int J Mol Sci* 2020;**21**(11).

[24] Yang G, Murashige DS, Humphrey SJ, James DE. A positive feedback loop between Akt and mTORC2 via SIN1 phosphorylation. *Cell Rep* 2015;**12**(6):937–43.

[25] Liu GY, Sabatini DM. mTOR at the nexus of nutrition, growth, ageing and disease. *Nat Rev Mol Cell Biol* 2020;**21**(4):183–203.

[26] Xu J-Y, Zhang C, Wang X, Zhai L, Ma Y, Mao Y, Qian K, Sun C, Liu Z, Jiang S, et al. Integrative proteomic characterization of human lung adenocarcinoma. *Cell* 2020;**182**(1):245–261.e17.

[27] Doll S, et al. Rapid proteomic analysis for solid tumors reveals LSD1 as a drug target in an end-stage cancer patient. *Mol Oncol* 2018;**12**(8):1296–307.

[28] Rodriguez H, Zenklusen JC, Staudt LM, Doroshow JH, Lowy DR. The next horizon in precision oncology: proteogenomics to inform cancer diagnosis and treatment. *Cell* 2021;**184**(7):1661–70.

[29] Wang Z, Liu G, Jiang J. Profiling of apoptosis- and autophagy-associated molecules in human lung cancer A549 cells in response to cisplatin treatment using stable isotope labeling with amino acids in cell culture. *Int J Oncol* 2019;**54**(3):1071–85.

[30] Chavez JD, Hoopmann MR, Weisbrod CR, Takara K, Bruce JE. Quantitative proteomic and interaction network analysis of cisplatin resistance in HeLa cells. *PloS One* 2011;**6**(5):e19892.

[31] Rocha CRR, Silva MM, Quinet A, Cabral-Neto JB, Menck CFM. DNA repair pathways and cisplatin resistance: an intimate relationship. *Clin (Sao Paulo Braz)* 2018;**73**(Suppl 1):e478s.

[32] Rudolph C, Melau C, Nielsen JE, Jensen KV, Liu D, Pena-Diaz J, Meyts ER, Rasmussen LJ, Jørgensen A. Involvement of the DNA mismatch repair system in cisplatin sensitivity of testicular germ cell tumours. *Cell Oncology (Dordrecht)* 2017;**40**(4):341–55.

[33] Wang G, Wang X, Xu X. Triptolide potentiates lung cancer cells to cisplatin-induced apoptosis by selectively inhibiting the NER activity. *Biomark Res* 2015;**3**:17.

[34] Chen P, Li J, Chen Y, Qian H, Chen Y, Su J, Wu M, Lan L. The functional status of DNA repair pathways determines the sensitization effect to cisplatin in non-small cell lung cancer cells. *Cell Oncol (Dordrecht)* 2016;**39**(6):511–22.

[35] Jackson SP, Bartek J. The DNA-damage response in human biology and disease. *Nature* 2009;**461**(7267):1071–8.

[36] Liu D, Dong C, Zeng L, Wu Z, Zhao P, Zhang L, Chen Z, Zou C. Epitranscriptomics and epiproteomics in cancer drug resistance: therapeutic implications. *Signal Transduct Targeted Therapy* 2020;**5**(1):193.

1058   STAT3 contributes to cisplatin resistance, modulating EMT markers, and the mTOR signaling in lung adenocarcinoma   **A.P. Morelli et al.**

Neoplasia Vol. 23, No. xxx 2021

[37] Kotsinas A, Aggarwal V, Tan E-J, Levy B, Gorgoulis VG. PIG3: a novel link between oxidative stress and DNA damage response in cancer. *Cancer Lett* 2012;**327**(1–2):97–102.

[38] Singh M, Hunt CR, Pandita RK, Yang C, Horikoshi N, Bachoo R, Serag S, Story MD, Shay JW, Powell SN, Gupta A, et al. Lamin A/C depletion enhances DNA damage-induced stalled replication fork arrest. *Mol Cell Biol* 2013;**33**(6):1210–22.

[39] Thakar T, Leung W, Nicolae CM, Clements KE, Shen B, Belinsky A, Moldovan G. Ubiquitinated-PCNA protects replication forks from DNA2-mediated degradation by regulating Okazaki fragment maturation and chromatin assembly. *Nat Commun* 2020;**11**(1):2147.

[40] Peter ME, Hadji A, Murmann AE, Brockway S, Putzbach W, Pattanayak A, Ceppi P. The role of CD95 and CD95 ligand in cancer. *Cell Death Differen* 2015;**22**(4):549–59.

[41] Pichon M-F, Labroquère M, Rezaï K, Lokiec F. Variations of soluble fas and cytokeratin 18-Asp 396 neo-epitope in different cancers during chemotherapy. *Anticancer Res* 2006;**26**(3B):2387–92.

[42] Liu H, Hu X, Zhu Y, Jiang G, Chen S. Up-regulation of SRPK1 in non-small cell lung cancer promotes the growth and migration of cancer cells. *Tumour Biol* 2016;**37**(6):7287–93.

[43] Wang C, et al. SRPK1 acetylation modulates alternative splicing to regulate cisplatin resistance in breast cancer cells. *Commun Biol* 2020;**3**(1):268.

[44] Pellarin I, Dall'Acqua A, Gambelli A, Pellizzari I, D'Andrea S, Sonego M, Lorenzon I, Schiappacassi M, Belleti B, Baldassarre G. Splicing factor proline- and glutamine-rich (SFPQ) protein regulates platinum response in ovarian cancer-modulating SRSF2 activity. *Oncogene* 2020;**39**(22):4390–403.

[45] Huynh J, Chand A, Gough D, Ernst M. Therapeutically exploiting STAT3 activity in cancer – using tissue repair as a road map. *Nat Rev Cancer* 2019;**19**(2):82–96.

[46] Huang S, Chen M, Shen Y, Shen W, Guo H, Gao G, Zou X. Inhibition of activated Stat3 reverses drug resistance to chemotherapeutic agents in gastric cancer cells. *Cancer Lett* 2012;**315**(2):198–205.

[47] Chen L, Zhang B, Shan S, Zhao X. Neuroprotective effects of vitexin against isoflurane-induced neurotoxicity by targeting the TRPV1 and NR2B signaling pathways. *Mol Med Rep* 2016;**14**(6):5607–13.

[48] Zulkifli AA, Tan FH, Putoczki TL, Stylli SS, Luwor RB. STAT3 signaling mediates tumour resistance to EGFR targeted therapeutics. *Mol Cell Endocrinol* 2017;**451**:15–23.

[49] Cui Y, Li Y, Zhang H, Wang F, Bau X, Li S. STAT3 regulates hypoxia-induced epithelial mesenchymal transition in oesophageal squamous cell cancer. *Oncol Rep.* 2016;**36**(1):108–16.

[50] Liang F, Ren C, Wang J, Wang S, Yang L, Han X, Chen Y, Tang G, Yang G. The crosstalk between STAT3 and p53/RAS signaling controls cancer cell metastasis and cisplatin resistance via the Slug/MAPK/PI3K/AKT-mediated regulation of EMT and autophagy. *Oncogenesis* 2019;**8**(10):1–15.

[51] Lin W-H, Chang Y, Hong M, Hsu T, Lee K, Lin C, Lee J. STAT3 phosphorylation at Ser727 and Tyr705 differentially regulates the EMT-MET switch and cancer metastasis. *Oncogene* 2021;**40**(4):791–805.

[52] Eiring AM, Page BDG, Kraft IL, Mason CC, Vallore NA, Resetca D, Zabriskie MS, Zhang TY, Khorashad JS, Engar AJ, Reynolds KR, et al. Combined STAT3 and BCR-ABL1 inhibition induces synthetic lethality in therapy-resistant chronic myeloid leukemia. *Leukemia* 2017;**31**(5):1253–4.

[53] Feng J, Jiang W, Liu Y, Huang W, Hu K, Li K, Chen J, Ma C, Sun Z, Pang X. Blocking STAT3 by pyrvinium pamoate causes metabolic lethality in KRAS-mutant lung cancer. *Biochem Pharmacol* 2020;**177**:113960.

[54] Gao S, Chen M, Wei W, Zhang X, Zhang M, Yao Y, Lv Y, Wang L, Zou X. Crosstalk of mTOR/PKM2 and STAT3/c-Myc signaling pathways regulate the energy metabolism and acidic microenvironment of gastric cancer. *J Cell Biochem* 2018;**120**(2):1193–202.

[55] Jin H-O, Lee Y, Park J, Kim J, Hong S, Kim H, Kim E, Noh WC, Kim B, Ye S, Chang YH, et al. Blockage of Stat3 enhances the sensitivity of NSCLC cells to PI3K/mTOR inhibition. *Biochem Biophys Res Commun* 2014;**444**(4):502–8.

[56] Wang Y, Tang F, Hu X, Zheng C, Gong T, Zhou Y, Luo Y, Min L. Role of crosstalk between STAT3 and mTOR signaling in driving sensitivity to chemotherapy in osteosarcoma cell lines. *IUBMB Life* 2020;**72**(10):2146–53.

[57] Wang J, Lv X, Guo X, Dong Y, Peng P, Huang F, Wang P, Zhang H, Zhou J, Wang Y. Feedback activation of STAT3 limits the response to PI3K/AKT/mTOR inhibitors in PTEN-deficient cancer cells. *Oncogenesis* 2021;**10**(1):8.

[58] Ternent T, Csordas A, Qi D, Goméz-Baena G, Beynon RJ, Jones AR, Hermjakob H, Vizcaíno JA. How to submit MS proteomics data to ProteomeXchange via the PRIDE database. *Proteomics* 2014;**14**(20):2233–41.